Shahrood University of Technology
Iranian Society of Mining Engineering (IRSME)
Journal of Mining and Environment (JME)
journal homepage: www.jme.shahroodut.ac.ir
THOMSON REUTERS

Stochastic Stability Analysis of Tunnels Considering Randomness of Rock Mass Properties

Masoud Mazraehli[1*], Shokroallah Zare[1] and Musa Adebayo Idris[2]

1. aculty of Mining, Petroleum and Geophysics Engineering, Shahrood University of Technology, Shahrood, Iran
2. Division of Mining and Geotechnical Engineering, Luleå University of Technology, Luleå, Sweden

Article Info

Received 20 October 2021
Received in Revised form 14 November 2021
Accepted 11 December 2021
Published online 11 December 2021

DOI:10.22044/jme.2021.11310.2113

Keywords

Underground excavations
Probabilistic stability analysis
Rock mass property variability
Finite difference method
Monte Carlo simulation

Abstract

The purpose of this work is to present an approach for the probabilistic stability analysis of tunnels considering the heterogeneity of geo-mechanical properties. A stochastic procedure is followed to account for the variability in the rock mass property characterization. The finite difference method is coupled with the Monte Carlo simulation technique to incorporate the randomness of rock mass properties. Moreover, a particular performance function is defined to investigate the excavation serviceability based on the permissible deformations. In order to validate the analysis, the probabilistic and the deterministic results are compared with the in-situ measurements. It can be observed that in both the probabilistic and deterministic analyses the largest displacements occur in the invert. In contrast, the smallest displacements are recorded in the sidewalls. Utilizing the performance function, the probability of failure for the invert, crown, left, and right wall is estimated as 100%, 68.8%, 16.2%, and 20.9%, respectively. Comparing the measured and calculated convergences, it is conjectured that the deterministic analysis underestimates the displacements, while the measured values are very close to the mean values predicted by the probabilistic analysis. The results obtained indicate that the presented approach could be a reliable technique compared to the conventional deterministic method.

1. Introduction

Stability analysis of underground excavations has been a research issue with a great interest in the geotechnical engineering for a long time. There are a large number of research works related to this topic, which can be divided into the deterministic [1-4] and probabilistic studies [5-15]. The deterministic methods have been widely used but the probabilistic studies are restricted in quantity [16-20]. Despite the popularity of the deterministic techniques in practice, these methods are unable to reckon with the inherent randomness of the geo-mechanical properties. The inherent randomness is one of the principal uncertainty sources in rock engineering, the others being the measurement and transformation error [21-23]. Ignorance of these uncertainties can remarkably influence the analysis results so that it may lead to applying too conservative safety factors in the design.

The probabilistic methods have been established in order to capture a more realistic perspective on how an over or under-estimate of response variables can affect the remedial requirements [24]. The Monte Carlo simulation (MCS), first-order (FORM), and second-order (SORM) reliability methods, point estimate method (PEM), response surface method (RSM), and artificial neural networks (ANN) might be utilized as the general scheme for the probabilistic analysis, though there are some differences in their applications. For instance, the methods can be classified into two classes considering rock mass heterogeneity [11]. In contrast to the other methods, MCS is categorized into a group that

Corresponding author: mazraehli.m@shahroodut.ac.ir (M. Mazraehli).

takes account of the rock mass property randomness.

In the recent years, MCS has started something like a scientific revolution. It is now practical to get an insight into how a problem solution is affected by the input parameter variation using the method [25]. In geotechnical engineering, MCS was first applied in many aspects such as the single random geo-mechanical variables (SRVs) [7, 13, 14]. Although these research works furthered the MCS applications in geotechnical engineering, they neglected the spatial randomness. Subsequently, some researchers have attempted to fill the gap by utilizing MCS coupled with the numerical software packages. Hsu and Nelson [26] have incorporated the distinct element method (DEM) and MCS in order to analyze the slope stability in a spatially variable weak rock mass. Idris and Nordlund [5] and Idris *et al*. [9-11] have used the finite difference method (FDM) to analyze the stability of underground mine stopes considering spatial variability. Yu *et al*. [24] have taken the advantage of stochastic numerical modeling in order to investigate the tunnel liner performance, concluding that the procedure could lead to a more equitable and economical design.

The above-mentioned studies established the MCS applications in modeling the inherent randomness of rock mass properties. There are, however, some aspects that still require more research works. Uncertainty in the distribution of the input parameters is one of these aspects that requires more surveillance. Tiwari *et al*. [13] have used PEM for the stability analysis of underground structures, while it is known that the implemented method only works with normally distributed functions. Analyzing a large number of geo-mechanical laboratory and field data, Mazraehli and Zare [27] have demonstrated that the distributions of rock mass properties do not necessarily follow the normal and log-normal distribution function rules. The stochastic numerical method was first adopted for the stability analysis of soil slopes. MCS was combined with the numerical analysis in order to introduce the spatially variable soil properties as the random field models [28-29]. Similar research works were carried out for rocks afterward [30-32]. Song *et al*. [31] have investigated the effect of spatial variability of rock mass properties on the ground deformation due to tunneling. Yu *et al*. [33] have evaluated the tunnel liner performance using the conditional and unconditional random field models. Zhang *et al*. [34] have compared the number of studies conducted in the field of spatial variability in different periods of time, stating that the topic has become more demanding over time. To the contrary, the main disadvantage of the random field method is that it requires the robust arithmetic capabilities to solve the matrices formed in each part of the modeling process.

Compared to the soil, a rock is a more complicated environment due to the effects of different parameters such as the strength properties (e.g. uniaxial compressive strength, elastic modulus, cohesion, friction, etc.), joint properties (e.g. roughness, spacing, and orientation), and weathering [8, 35-37]. This imposes some more computational difficulties on the probabilistic studies, which, in turn, suffer from time-consuming mathematical solutions. It is, therefore, necessary to present a stochastic modeling scheme, which necessitates a lower computational effort. This paper presents such a procedure for the probabilistic tunnel stability analysis, in which there is no need for intensive mathematical formulations. Based on the geological strength index (GSI), a probabilistic methodology is used to obtain the statistics of the rock mass strength and deformation parameters. Then a Fish function is applied to compose the MCS and the FDM methods in FLAC to take account of the spatial rock mass variability. Moreover, a particular performance function is defined based on the critical and permissible deformation of the tunnel in order to analyze the probability of failure (PoF).

2. Probabilistic numerical modeling

2.1. Random property assignment procedure

Since the random field method requires the cumbersome decomposition of matrix relations, it was tried to implement an approach that does not require to solve the problematic relationships. Accordingly, the MCS method was implemented in FLAC using a FISH function. FISH is a scripting language embedded within the software to define new variables and functions [38]. The scripted function involves an iterative process of assigning random variables to the numerical zones.

A schematic illustration of the property assignment process is shown in Figure 1. Having a dimension of 70*70 ($l = 70\,m$), the model contains 78400 finite-difference zones (280 zones in both the x and y directions). It means that each zone has a side length of 0.25 m. As a result, it provides an acceptable resolution for a random

property mapping and also a reasonable numerical accuracy. Each model realization might be specified by a matrix in the form of $[z_{ij}]_{280\times280}$, where z_{ij} represents a zone located in the ith row and jth column whose centroid coordinates are distinguished by:

$$x_i = l/(n+1) + i.sl \quad i = 0,1,2,\dots,279 \tag{1}$$

$$y_j = l/(n+1) + j.sl \quad j = 0,1,2,\dots,279 \tag{2}$$

where sl is the side length of each zone, and $n+1$ represents the number of zones in the horizontal or vertical direction. After determination of the zone centroid, random properties are assigned to the corresponding zones denoted by z_{ij}. To this end, the zones are selected randomly using the following equations:

$$k = int\left((i).urand\right) + 1 \quad kcount \leq \text{number of calculated class zones} \tag{3}$$

$$l = int\left((j).urand\right) + 1 \quad lcount \leq \text{number of calculated class zones} \tag{4}$$

where the pair (k,l) shows a zone located in the kth row and lth column. The zone is selected randomly to assign its property variables based on a certain property class. The function int rounds the product of i and $urand$ to its nearest integer, while $urand$ is a stochastic uniform value between 0 and 1. The procedure continues until the number of the pairs ($kcount$ and $lcount$) approaches the class zone quantity (a-f in Figure 1).

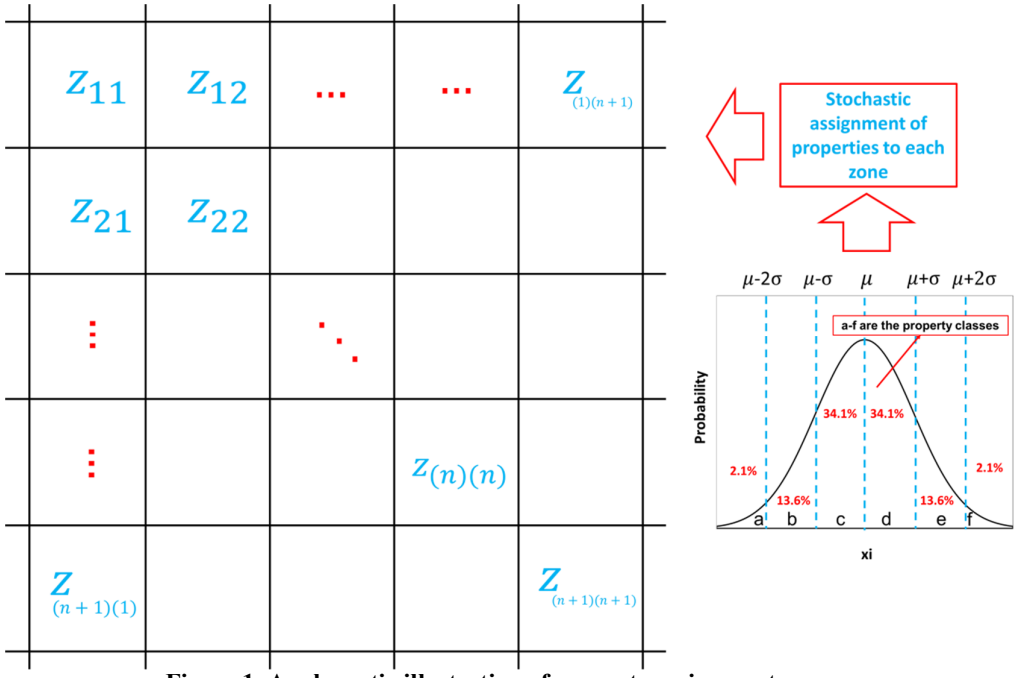

Figure 1. A schematic illustration of property assignment process.

The process of random property realization can be summarized as follows:

1- Construction of the model grid with $n+2$ nodes in both the x and y directions.

2- Determination of the zone centroid coordinates (x_i, y_i) using Equations (1) and (2).

3- Calculation of the proportional frequency for every property class of the variables.

4- Assigning the mean values of the properties based on their distribution functions to all numerical zones.

5- Allocating the random numerical zones using Equations (3) and (4).

6- Assigning the values that belong to the other classes (weaker or stronger than the mean) to the specified zones in the last step.

7- Repeating steps 5 and 6 to a point that all the zones are assigned.

8- Repeating steps 1 to 7 to a point that the quantity of simulations does not significantly affect the response required.

In this regard, each realization corresponds to a possible arrangement of the geo-mechanical properties of the ground. Moreover, the average values for the model parameters remain very close to the mean values using the procedure. Furthermore, analyzing a large number of realizations would result in a preferable perspective on the tunnel response.

This work is focused on the uncertainty of the geo-mechanical properties, while the discontinuities are the other aspects of uncertainty in rock engineering. The effect of discontinuities is implicitly considered in the GSI used for the rock mass classification purposes. On the other hand, it is also possible to take the discontinuity effect into account in an explicit way utilizing the stochastic modeling techniques such as discrete fracture network (DFN). Based on the literature, the discontinuities cause some irregularities in stress and displacement distribution so that the larger displacements occur adjacent to these structures [39-41].

2.2. Case study and modeling specifications

The Alborz twin tunnels include an essential part of the Tehran-North expressway with 6300 m length in each direction [42]. Figure 2 presents the longitudinal profile of the tunnel. According to the profile, the studied section is located in the Shemshak formation, close to the north portal (chainage 0 + 293.20 m). The formation mainly consists of the argillite and sandstone sequences with coal lenses and dacite dykes. The highest uniaxial strength values are associated with the dacite samples, while the median and the lowest are related to the sandstone and the argillite samples, respectively. Furthermore, the groundwater condition is in the form of dripping (e.g. 0.1 to 0.3 L/s) in this section. Table 1 summarizes the physical parameters (i.e. unit weight denoted by γ, and overburden denoted by H) of the studied section.

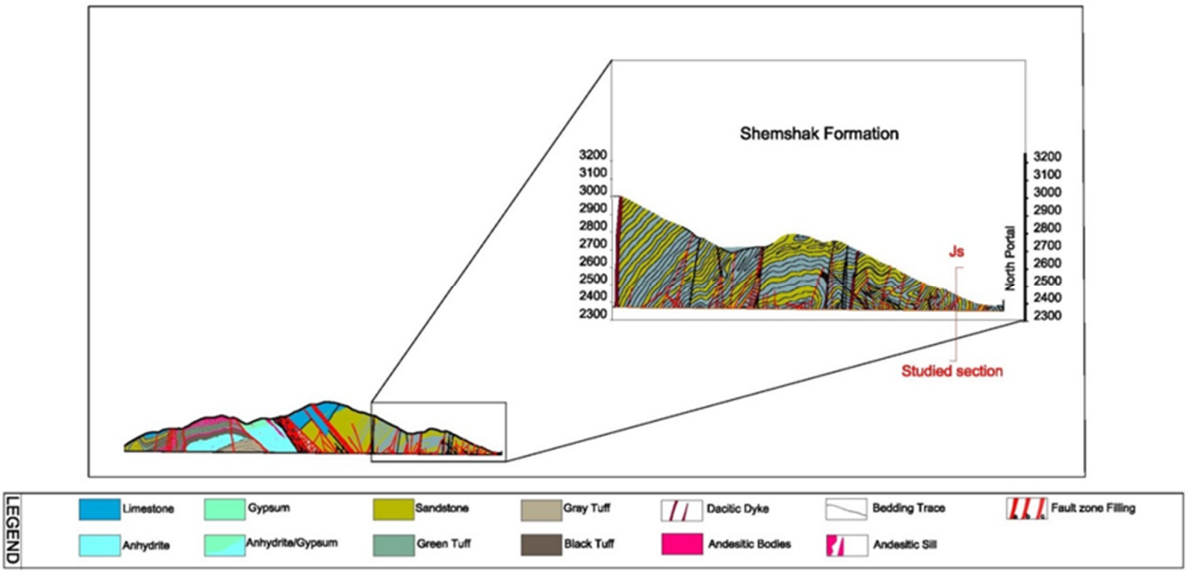

Figure 2. Longitudinal profile of Alborz twin tunnels [42].

Table 1. Physical parameters of the section [42].

Geological unit	Symbol	Chainage (km)	γ (kN/m^3)	H (m)
Shemshak	*Js*	0 + 293.20	26.3	65

A square FDM model with a 70 m side length was built using FLAC. The roller and fixed boundary conditions were applied to different boundaries of the model. The upper boundary was fixed against the displacements in the y direction, while the displacements of the other sides of the model were fixed in both the x and y directions. The model geometry and boundary conditions are illustrated in Figure 3(a). Before modeling the tunnel excavation, the in-situ stress state was balanced.

The field stresses for the studied section were set, defining a constant hydrostatic in-situ stress field ($k = 1$) as follows:

$$\sigma_v = \sigma_h = \gamma . H = 1.71 \text{ MPa} \quad (5)$$

where γ and H are the unit weight of rock and the overburden height, respectively. In the case of the plane-strain condition, the out of plane stress is calculated as (consider Poison's ratio $\vartheta = 0.3$):

$$\sigma_z = \vartheta(\sigma_v + \sigma_h) = 1.03 \text{ MPa} \quad (6)$$

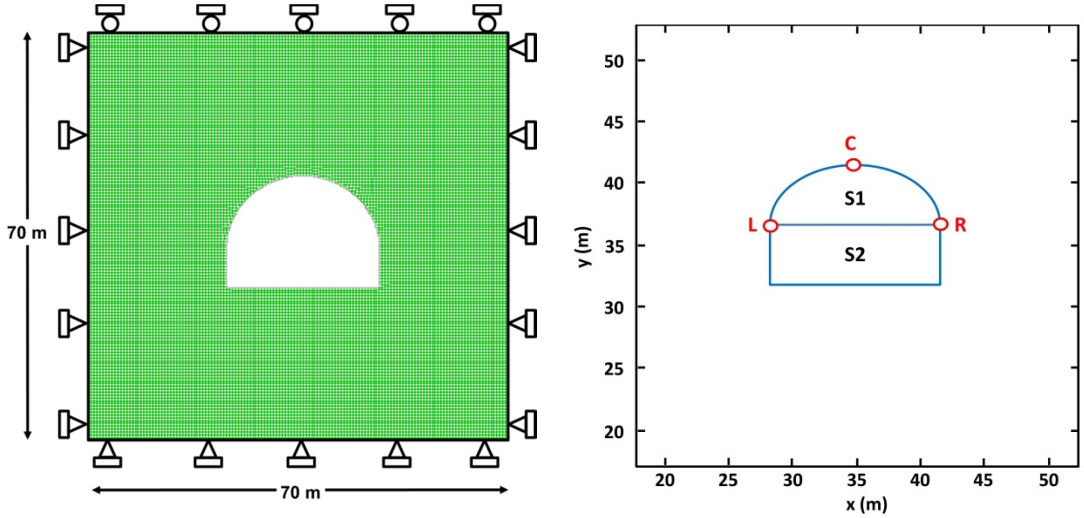

(a) (b)

Figure 3. a) Boundary conditions and model geometry; b) excavation sequences (S1 and S2) and measurement points (C, L, and R).

The sequential excavation method is being utilized in the construction phase through the top-heading and bench technique (i.e. two stages). The top-heading of the tunnel is in the form of an arc with a diameter of 13 m, and the square-shaped bench has a side length of 3.3 m with a total tunnel height of 9.8 m. Three numerical monitoring points were selected based on the predefined measurement points on the crown and sidewalls. Figure 3(b) shows the excavation sequences and measurement points.

Figure 4 demonstrates a sample of random realizations of the geo-mechanical properties. In order to achieve an acceptable level of accuracy, it is expected to run thousands of numerical simulations. It is, however, possible to determine the optimum number of simulations by comparing the calculated mean values and standard deviations.

3. Probabilistic rock mass properties calculation

In order to characterize the rock mass properties, the required geo-mechanical parameters were obtained based on the available information. The results of engineering geological field mapping were used to estimate the distribution functions of the rock mass properties. The implemented procedure for rock mass characterization (based on the statistical parameters of the intact rock and discontinuities) is presented in this section.

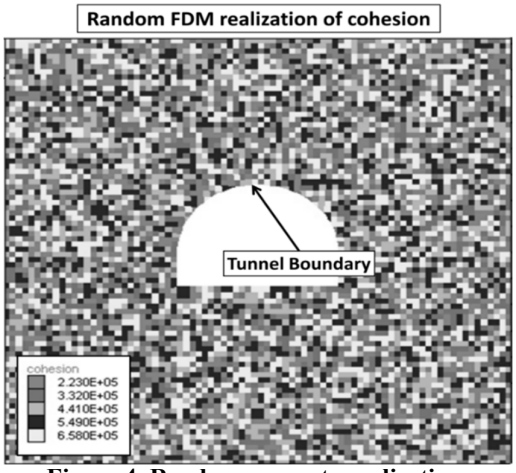

Figure 4. Random property realization.

3.1. Formulation of rock mass property estimation

The perfectly elastic-plastic constitutive model was used to model the plastic behavior of rock mass. The rock mass obeys the Mohr-Coulomb failure criterion for which the cohesive strength and internal friction angle are derived based on the Hoek-Brown constants (m_b, s, and a). Hoek

et al. [43] and Hoek and Brown [44] have proposed Equations (7)-(9) based on GSI and intact rock constants:

$$m_b = m_i \exp\left(\frac{GSI - 100}{28 - 14D}\right) \quad (7)$$

$$s = \exp\left(\frac{GSI - 100}{9 - 3D}\right) \quad (8)$$

$$a = \frac{1}{2} + \frac{1}{6}\left(e^{-GSI/15} - e^{-20/3}\right) \quad (8)$$

The parameter D in Equations (7)-(9) denotes the factor of disturbance, which depends on the significance of blasting and stress relaxation experienced by the rock mass (a value between 0 for undisturbed rock mass and 1 for completely disturbed rock mass). In this project, a pilot tunnel was excavated utilizing an open gripper TBM for geological engineering mapping [42]. Hence, the parameter was considered as 0 due to the absence of blasting operation during the data collection process.

After calculating the constants, it is possible to determine the uniaxial compressive strength of the rock mass using the following relationship [43]:

$$\sigma_{cm} = \sigma_c s^a \quad (10)$$

The tensile strength of the rock mass could then be determined from Equation (11) as follows:

$$\sigma_{tm} = \frac{s\sigma_c}{m_b} \quad (11)$$

The deformation modulus of the rock mass might be specified using the following equation [35, 44]:

$$E_m = 10^5 \left(\frac{1 - D/2}{1 + e^{((75+25D-GSI)/11)}}\right) \quad (12)$$

In the next step, it would be possible to calculate the strength parameters of the Mohr-Coulomb criterion (c and ϕ) using Equations (13) and (14) [43]:

$$\phi = \sin^{-1}\left[\frac{6am_b(s + m_b\sigma_{3n})^{a-1}}{2(1+a)(2+a) + 6am_b(s + m_b\sigma_{3n})^{a-1}}\right] \quad (13)$$

$$c = \frac{\sigma_{ci}[(1+2a)s + (1-a)m_b\sigma_{3n}](s + m_b\sigma_{3n})^{a-1}}{(1+a)(2+a)\sqrt{\frac{1 + (6am_b(s + m_b\sigma_{3n})^{a-1})}{(1+a)(2+a)}}} \quad (14)$$

where ϕ and c are the friction angle and cohesion, respectively, and $\sigma_{3n} = \sigma_{3max}/\sigma_{ci}$.

3.2. Determination of probability distribution functions

Many researchers have approved that the distributions of rock testing results might be well-described by the normal distribution functions [22, 46-52]. In this paper, since there is no adequate amount of data required for conducting the statistical analysis, PDFs were selected based on the suggestions made by Cai [8] for the intact rock. It was, therefore, decided to use the normal distribution functions for all of the intact rock variables.

Table 2 presents the statistical parameters of the intact rock properties, namely their mean values and standard deviations. Furthermore, the corresponding PDFs are shown in Figure 5. It is worth noting that the standard deviation values were determined based on the differences between the property values with the accumulative frequency of 49.9 (i.e. the mean value) and 15.8%.

Table 2. Intact rock properties.

Characteristic	Statistic	Value
Hoek-Brown constant m_i	Mean	13
	Standard deviation	2.0
	PDF	Normal
Uniaxial compressive strength (MPa)	Mean	81
	Standard deviation	23.6
	PDF	Normal

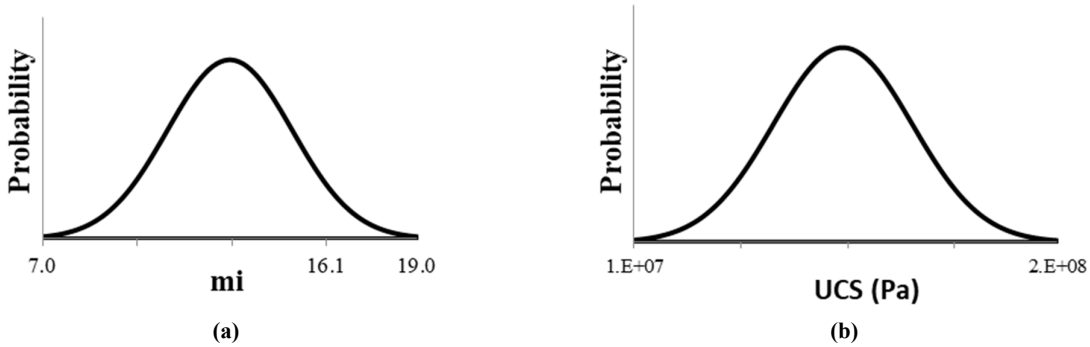

Figure 5. Probability distribution curves for: a) m_i; b) uniaxial compressive strength of intact rock.

As mentioned above, Mazraehli and Zare [27] have proposed appropriate coefficients of variation and PDFs for the rock mass properties that were considered in the current study. Combining the above-mentioned formulation and MCS, it would be possible to characterize the rock mass (Table 3). Figure 6 presents the simulation results together with their probability distribution curves. Lognormal distribution was used for the Hoek-Brown constant a, σ_{tm}, and E_m. On the other hand, it was shown that the Gamma distribution was the best-fitted probability function for m_b, s, and σ_{cm} [27]. The results obtained also indicate that both c and ϕ (i.e. strength parameters) are related to the normal distribution functions. According to the figure, a has the lowest dispersion around its mean, for which the coefficient of variation equates to almost 2%. It should be noted that the algorithm is restricted not to generate negative parameters since the geo-mechanical properties are non-negative (see Figure 6(b)).

Table 3. PDFs and their statistical parameters of rock mass characteristics.

Characteristic	Statistic	Value
m_b	Mean	1.03
	Standard deviation	0.45
	PDF	Gamma
s	Mean	0.001
	Standard deviation	0.002
	PDF	Gamma
a	Mean	0.51
	Standard deviation	0.01
	PDF	Lognormal
σ_{cm} (MPa)	Mean	2.332
	Standard deviation	1.612
	PDF	Gamma
E_m(GPa)	Mean	2.027
	Standard deviation	1.569
	PDF	Lognormal
σ_{tm} (MPa)	Mean	0.750
	Standard deviation	0.633
	PDF	Lognormal
c (MPa)	Mean	0.440
	Standard deviation	0.109
	PDF	Normal
ϕ (°)	Mean	40.190
	Standard deviation	4.360
	PDF	Normal
GSI	Mean	45
	Standard deviation	8.300
	PDF	Normal

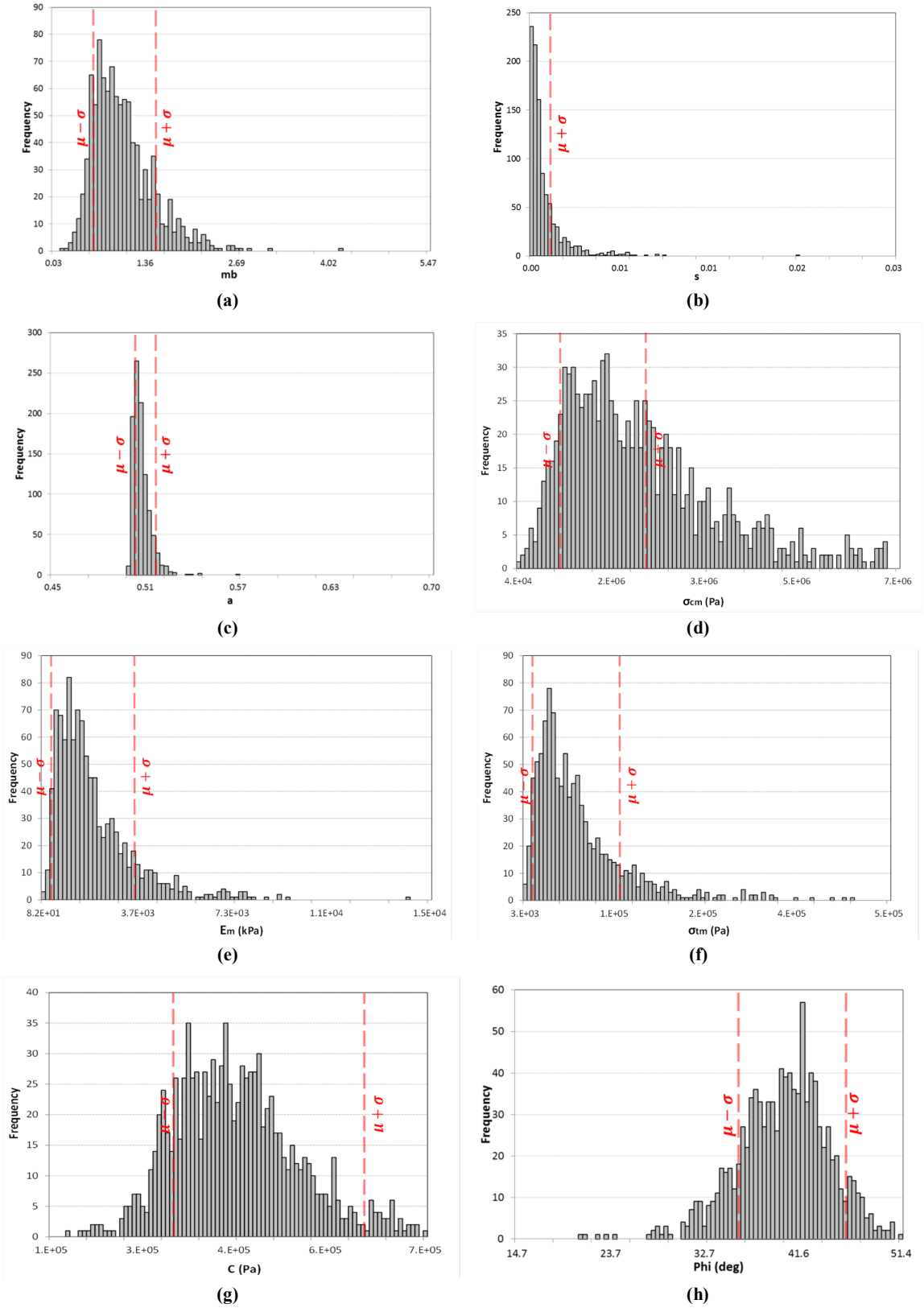

Figure 6. Distribution histograms for: a) m_b; b) s; c) a; d) σ_{cm}; e) E_m; f) σ_{tm}; g) c; h) ϕ.

4. Results and Discussion

Displacements of the tunnel walls were considered the deciding factors for analyzing the tunnel response to the in-situ ground condition rather than the yield zone depth. It was chosen because concrete was planned to be installed as the final support system instead of a systematic rock-bolt network. In the case of rock-bolts, an analysis based on the yield zone extent around the tunnel would be more efficient to decide their lengths and network density.

One thousand random realizations were run to represent the intrinsic randomness of the geo-mechanical properties. The total displacement vectors around the tunnel for one of the realizations are illustrated in Figure 7. The displacement vectors in the figure represent the values calculated after the complete excavation of the last stage in a stochastic numerical model. It can be seen that the displacement magnitudes are higher in the tunnel invert compared to the sidewalls and the crown. This issue can be related to the unit stress factor and the sharp corners of the tunnel in the invert part. The maximum displacement was recorded as 47.88 mm. The results obtained were integrated and interpreted to get distributions of displacements and their statistical parameters (i.e. mean value and standard deviation).

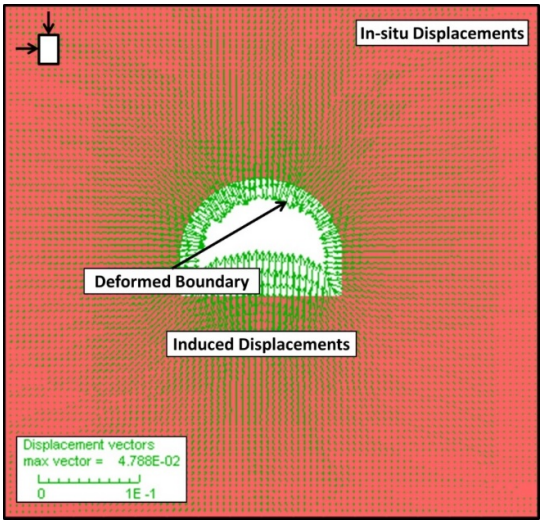

Figure 7. Total displacement vectors around excavation for one of the realizations.

PDFs of the total displacement in different parts of the tunnel section are presented in Figure 8. The mean values of displacement in the right wall, left wall, crown, and invert were 19.14 mm, 19.47 mm, 22.25 mm, and 42.32 mm, respectively. Moreover, their standard deviations were equal to 2 mm for the first three parameters and 3 mm for the latter. It would then be possible to calculate the coefficient of variation for the parameters using Equation (15).

$$c_v = \frac{\sigma}{\mu} \quad (15)$$

where σ is the standard deviation, and μ denotes the mean value. For the above-mentioned displacements, the coefficients of variation were calculated as 10%, 10%, 9%, and 7%, respectively.

4.1. Permissible strain limits

After estimating the statistical parameters, it is required to implement a criterion for analyzing the tunnel stability. Most of the published works utilize plastic zone thickness around the tunnel as the desired response parameter. It is, however, clear that the variable cannot be beneficial enough for a concrete support design. On the other hand, the critical strain concept [53] might be used as a control tool for the stability analysis of concrete tunnels. The concept was developed for tunnel design applications in order to estimate the rock mass deformation before failure [44]. Afterward, this method was revised by Li and Villaescusa [54]. The critical strain (ε_c in Equation (16)) is defined as the ratio of maximum compressive strength to initial tangent deformation modulus [55].

$$\varepsilon_c = \frac{\sigma_{cm}}{E_m} \quad (16)$$

where σ_{cm} and E_m are the rock mass strength and the deformation modulus, respectively. According to the values presented in Table 4, the average critical strain was obtained as 0.11%. The permissible strain (ε_a) might then be determined using Equation (17) [8]:

$$\varepsilon_a = \frac{\varepsilon_c}{1-R_a} \quad (17)$$

where R_a is a parameter representing the failure strength, and can be assumed to be 0.60, 0.65 or 0.70 based on the generalized crack initiation and propagation thresholds [8]. The permissible displacement (U) was determined using Equation (18) as follows:

$$U = \varepsilon_a . r \quad (18)$$

where r is the equivalent radius of the tunnel, and can be calculated from the following relationship:

$$r = \frac{d}{2} = \frac{(H+W)}{4} \quad (19)$$

where d, H, and w denote the tunnel diameter, height, and width, respectively. Thus the equivalent tunnel radius or so-called normalization dimension was estimated as $(13 + 9.8)/4 = 5.7$ m.

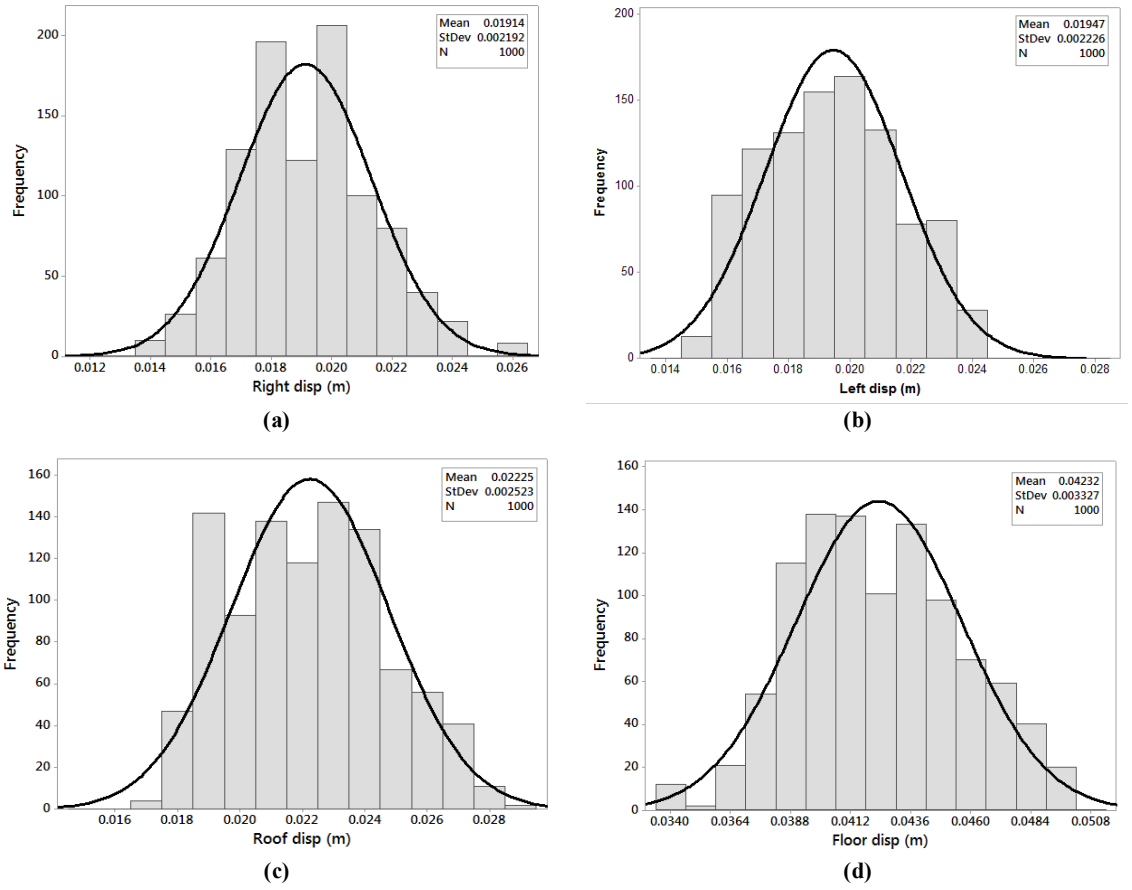

Figure 8. Probability density function of total displacement in: a) right wall; b) left wall; c) crown; d) invert.

4.2. Performance function

The tunnel excavation results in the disturbance of the in-situ stress state around the underground space [56]. The new stresses in the rock masses surrounding the tunnel are called the induced stresses. If these stresses exceed a certain level, they cause excavation failure and its loss of serviceability.

It is required to define a performance function to investigate the serviceability of the tunnel. This function was used here to determine PoF, and it was defined as follows:

$$g(x) = U - R(x) \quad (20)$$

where U and $R(x)$ are the average permissible displacement and the model displacement variable, respectively. When the performance function becomes negative ($g(x) < 0$), it implies that the corresponding model displacement exceeds the permissible limit, and a failure event is probable. Contrarily, when $g(x) > 0$, the tunnel would be stable, and its performance is desirable. The limit state surface is also defined by $g(x) = 0$, which is the boundary between the unstable and the stable conditions. Finally, PoF (i.e. instability of the tunnel) might be defined as:

$$P_f = P[g(x) < 0] = \int f(x)dx \quad (21)$$

for $g(x) < 0$

The right-hand side of Equation (19) means that PoF can be estimated from the area below the PDF curve of displacement beyond a vertical line specified by the limit state (Figure 9).

4.3. Probability of failure (PoF)

The permissible strain values would be calculated as 0.27%, 0.31%, and 0.37%, while the allowable displacements were obtained as 15.39 mm, 17.67 mm, and 21.09 mm for different residual strength parameters (U_{max} = 21.09 mm). The obtained critical and permissible displacement values are presented and compared in Table 4. It can be observed that the mean value of displacement in the tunnel invert (i.e. maximum averaged model displacement) is more than two times the allowable displacement. There is, therefore, an immediate need for taking remedial actions in the floor part to maintain the tunnel stability. The estimated PoFs for different parts are presented in Figure 10. PoFs for the right and left walls are different due to the slight variation in their mean and standard deviation. Since the modeled invert displacements are higher than the permissible limit, its PoF is 100%. Furthermore, PoF for the crown is ranked second with 68.8%. Table 5 presents the detailed results, which contain the mean values, standard deviations, and PoFs.

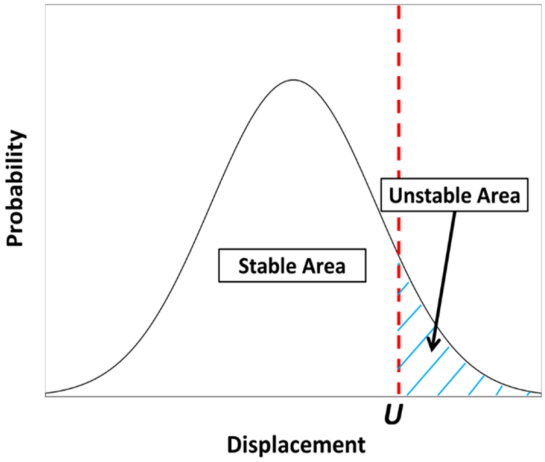

Figure 9. Estimation of PoF.

Table 4. Permissible and measured displacements and strains.

Residual strength parameter	Critical strain (%)	Permissible strain (%)	Permissible displacement (mm)	Maximum averaged model displacement (mm)
0.60	0.11	0.27	15.39	42.32
0.65		0.31	17.67	
0.70		0.37	21.09	

Table 5. Probabilistic stability analysis results.

	Statistics of model displacement			Maximum permissible displacement (mm)	PoF (%)
	Mean (mm)	S.D. (mm)	COV (%)		
Right wall	19.14	2	10	21.09	16.2
Left wall	19.47	2	10		20.9
Crown	22.25	2	9		68.8
Invert	42.32	3	7		100

4.4. Tunnel monitoring

It is essential to utilize the monitoring techniques in the underground excavations during construction and service periods in order to control and investigate the ground behavior. The Alborz tunnel was instrumented to monitor the inward tunnel deformation by use of the convergence pins and extensometers. As discussed earlier, the tunnel excavation brings about wall displacements. The convergence pins are the most common tools used for tunnel movement measurement, which evaluate the relative displacement of two points on the excavation boundary [57]. The advantages of this method are its facility in use, high measurement rate, and low cost. A set of instruments was installed in the chainage. Figure 11 depicts the instruments, their installing locations, and the monitoring results. The final relative convergence values were selected after smoothness of the displacements. According to the figure, the relative displacements were equal to 4 mm for the hypothetical line connecting the left and the right walls (L-R) and 3 mm for the crown to both the right wall (C-R) and the left wall (C-L). The numerical and measured convergence values are compared in Table 6. The mean numerical convergences are in good accordance with the relative displacements recorded by the monitoring instruments (after the face being far enough from the station). It must be noted that the accuracy of the monitoring tool was in mm but the numerical displacements were calculated in 0.01 mm.

Table 6. Calculated and measured relative displacements at chainage 0 + 293.20.

Location	Measured displacements (mm)			Calculated displacements (mm)		
	L-R	C-R	C-L	L-R	C-R	C-L
Eastern tunnel	4.00	3.00	3.00	3.84	3.11	2.78

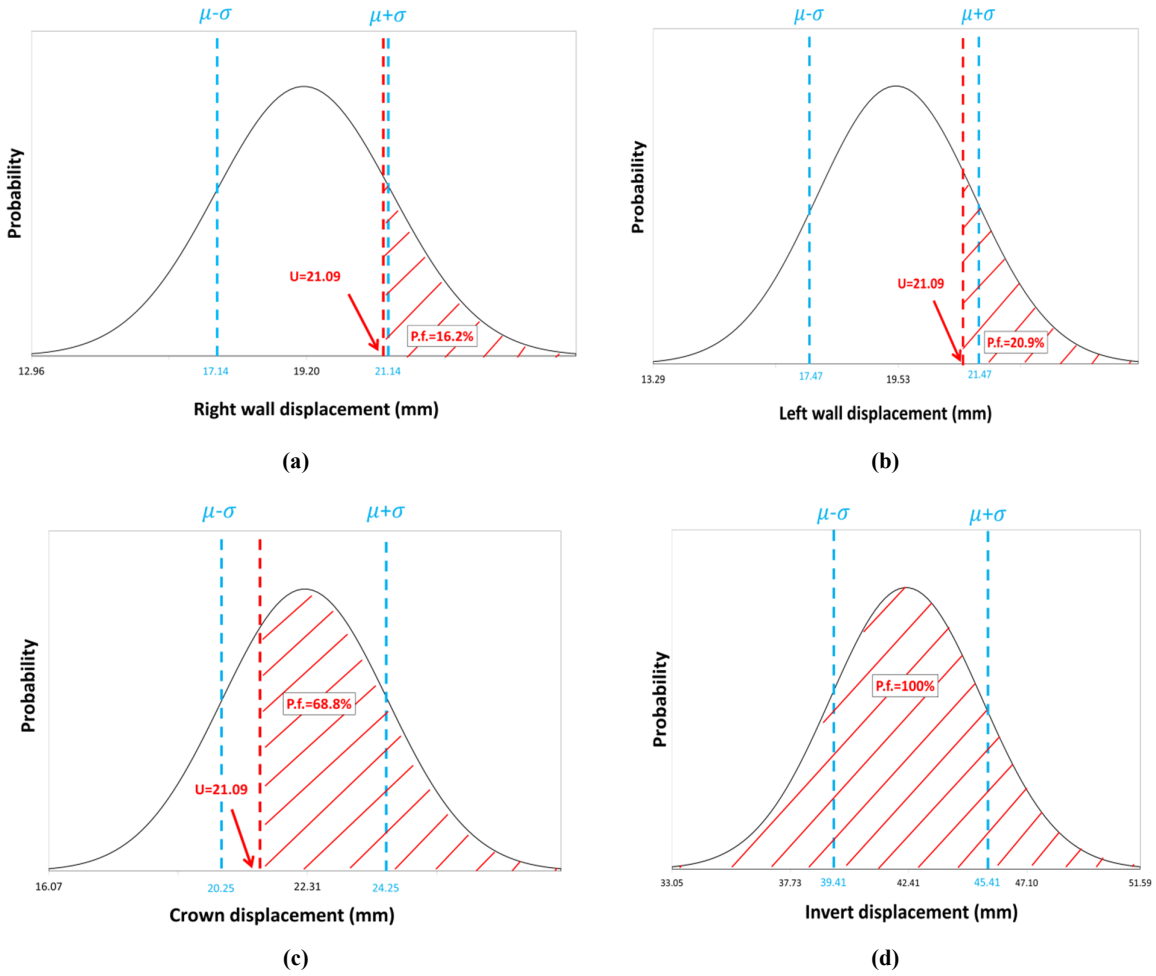

Figure 10. PoF for: (a) right wall; (b) left wall; (c) crown; (d) invert.

4.5. Comparing probabilistic and deterministic analysis results

In this section, the probabilistic results are compared with the deterministic ones. The mean values were used as the input parameters for the deterministic model. The other specifications (e.g. failure criterion, boundary, initial conditions, etc.) were the same. The details of numerical modeling were described in the previous sections. Figure 12 compares the results obtained from the deterministic and probabilistic analyses, which are provided in Table 7. The mean values from the probabilistic method were used to compare with the deterministic results. It can be observed that the deterministic displacements are smaller than the probabilistic values. It is, therefore, clear that employing this technique would result in a non-realistic estimation of the tunnel deformation. Consequently, the displacements fall behind the permissible limit, and one might conclude that the tunnel will be stable without a significant support system installation.

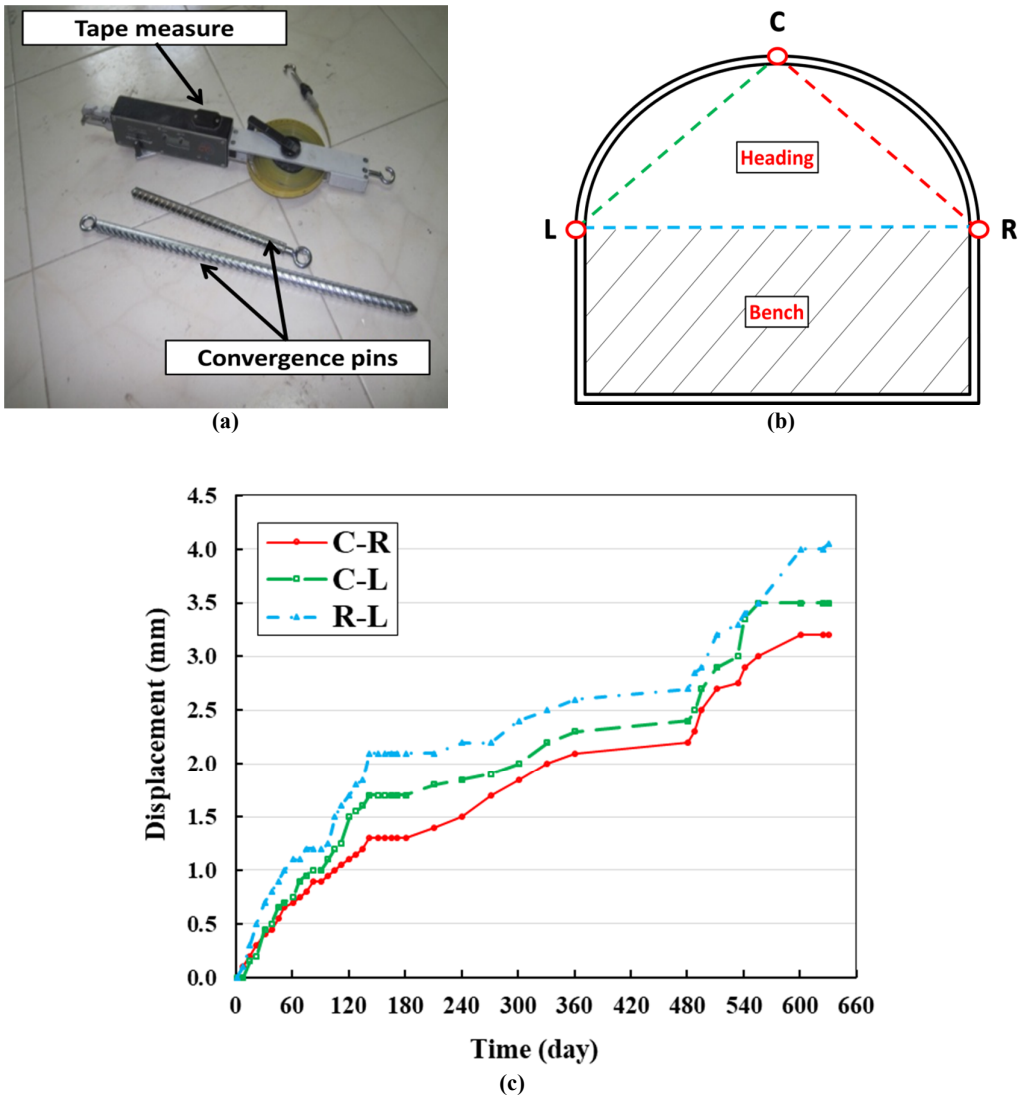

Figure 11. a) Instruments; b) pin locations; c) monitoring results.

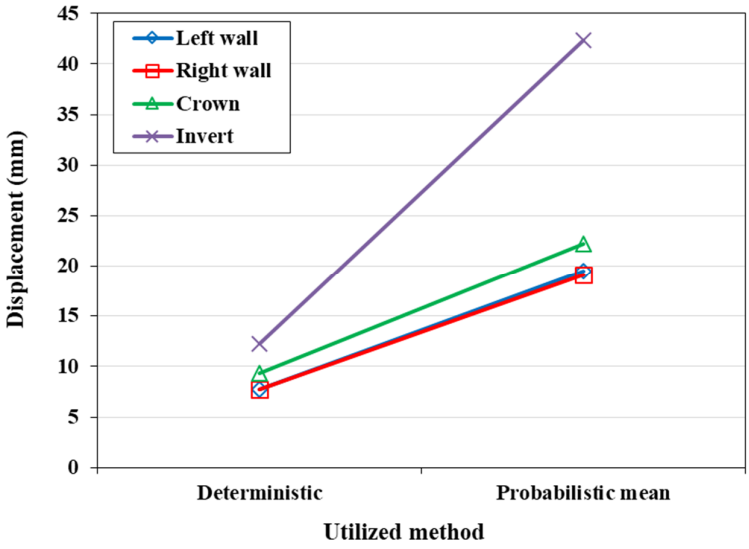

Figure 12. Comparison of deterministic and probabilistic displacements.

Table 7. Comparing deterministic and probabilistic stability analysis results.

	Deterministic displacement (mm)	Mean probabilistic displacement (mm)
Right wall	7.77	19.14
Left wall	7.76	19.47
Crown	9.33	22.25
Invert	12.28	42.32

Figure 13 compares the deterministic, probabilistic, and measured convergences. As discussed above, the deterministic displacements are far from the probabilistic means and measured values. It is also shown that the crown convergences to the both sidewalls are almost identical using three methods (C-R and C-L). Adversely, the sidewall convergences were obtained to be different (L-R). In this case, the deterministic analysis revealed its inefficiency again. In contrast, the probabilistic values were very close to the measured displacements.

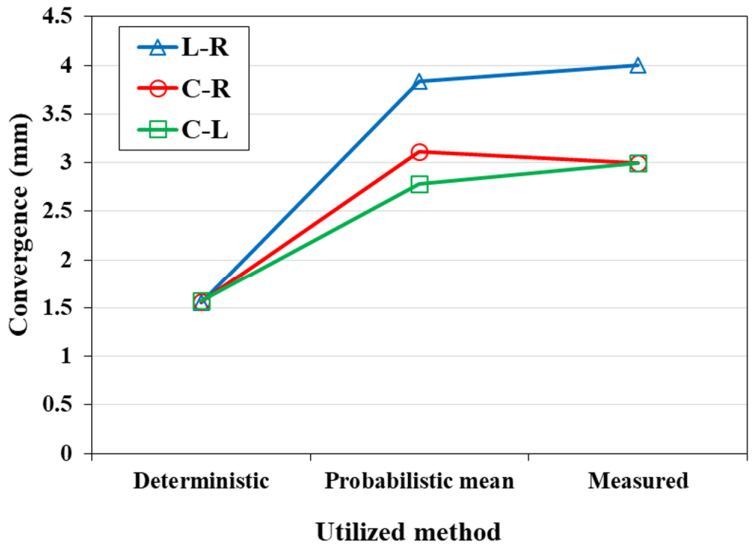

Figure 13. Comparison of deterministic, probabilistic, and measured convergences.

4.6. Support system requirements

Site investigations for the conventional rock mass characterization are not often accurate enough to get its quality into perspective during the design stage. It would be possible to select the stabilization measures and the support system requirements after overlapping different data sources gathered during the comprehensive site characterization, the numerical modeling results and interpretation, and the observations during the construction stage.

The most common brittle failure modes are cracking, spalling, slabbing, and collapse [58], while squeezing and swelling could be categorized in the ductile class [59]. During the construction stage, there was no vital instability, and the partial rock-falls and minor spalling were the only observed hazards. Therefore, a preliminary support system consisting of a shotcrete layer with 15 cm thickness and non-systematic rock bolting was considered to be sufficient for this section. The analyses, however, showed the possibility of exceeding the permissible displacement in the crown and invert. Table 8 illustrates that the excavation behavior falls in the third class of the H1 geo-mechanical hazard group. According to Russo [59], it corresponds to the Ma1 and Mb5 stabilization measures, which require the actions presented in Table 9. It is, therefore, recommended to utilize a composition of steel sets, steel fiber-reinforced shotcrete (SFRS), and rock-bolts as the final support system in this section.

Table 8. Rationale used for selection of support system based on Russo [59].

Prevalent hazard		RMR	Excavation behavior	Typical mitigation measures
H1	Wedge instability/Rockfall	> 80	Stable rock mass with the only possibility of local rock block fall; rock mass of very good quality with elastic response upon excavation	Ma1-Mb3
		61-80	Rock wedge instability; rock mass of good quality with elastic response upon excavation	Ma1-Mb3
		41-60	Pronounced tendency to rock-fall; rock mass of fair quality, with possible occurrence of a moderate development of plastic zone	Ma1-Mb5

Table 9. Proposed tunnel stabilization measures based on Russo [59].

Code	**a) In advancement to excavation**
Ma1	Controlled drainage ahead of tunnel face/contour
	b) During excavation
Mb5	Confinement by a differently composed system (steel ribs, fbr shotcrete, bolts, …)

5. Conclusions

In this work, we presented a methodology for the stochastic stability analysis of rock tunnels. The spatial variability of rock mass properties was considered using the stochastic finite difference method. The Monte Carlo simulation technique was utilized for developing the model realizations. Besides, the deterministic numerical analysis was also performed for the comparison purposes. Furthermore, the critical strain concept and the tunnel displacements were used to define the tunnel performance function. The numerical results were compared with the in-situ measurements in order to check the validity of the results. Subsequently, the support requirements of the tunnel were proposed. According to the results obtained, the following conclusions could be drawn for the conducted work:

- The probabilistic mean convergences were in good accordance with the measured values in the monitoring points.
- Compared to the in-situ measurements, the deterministic analysis underestimates the displacements. In contrast, the probabilistic mean values are close to the measured convergences.
- Employing the permissible displacement concept would make the tunnel performance function more comprehensible.
- Based on the observations and the results obtained, it is recommended to utilize a composition of steel sets, steel fiber-reinforced shotcrete, and rock bolts as the final support system of the tunnel section.
- Compared to the random field method, the presented approach obtains reliable results with a lower computational effort.

Acknowledgments

The authors would like to express their grateful appreciation to Geodata Engineering SpA and Tehran-Shomal Freeway Company for providing the required data during the work.

References

[1]. Pelizza, S., Oreste, P., Peila, D., and Oggeri, C. (2000). Stability analysis of a large cavern in Italy for quarrying exploitation of a pink marble. Tunnelling and underground space technology. 15 (4): 421-435.

[2]. Zhu, W., Li, S., Li, S., Chen, W. and Lee, C. (2003). Systematic numerical simulation of rock tunnel stability considering different rock conditions and construction effects. Tunnelling and underground space technology. 18 (5): 531-536.

[3]. Chehade, F. H., and Shahrour, I. (2008). Numerical analysis of the interaction between twin-tunnels: Influence of the relative position and construction procedure. Tunnelling and underground space technology. 23 (2): 210-214.

[4]. Funatsu, T., Hoshino, T., Sawae, H., and Shimizu, N. (2008). Numerical analysis to better understand the mechanism of the effects of ground supports and reinforcements on the stability of tunnels using the distinct element method. Tunnelling and Underground Space Technology. 23 (5): 561-573.

[5]. Idris, M. A., and Nordlund, E. (2019). Probabilistic-Based Stope Design Methodology for Complex Ore Body with Rock Mass Property Variability. Journal of Mining Science. 55 (5): 743-750.

[6]. Jiale, H., and Xiaohong, L. (2021). Reliability analysis considering spatial variability by combining spectral representation method and support vector machine. European Journal of Environmental and Civil Engineering. 25 (6): 1136-1157.

[7]. Behnia, M., and Seifabad, M. C. (2018). Stability analysis and optimization of the support system of an underground powerhouse cavern considering rock mass variability. Environmental Earth Sciences. 77 (18): 1-16.

[8]. Cai, M. (2011). Rock mass characterization and rock property variability considerations for tunnel and cavern design. Rock mechanics and rock engineering. 44 (4): 379-399.

[9]. Idris, M. A., Saiang, D., and Nordlund, E. (2011). Numerical analyses of the effects of rock mass property variability on open stope stability. In 45th US Rock Mechanics/Geo-mechanics Symposium, OnePetro.

[10]. Idris, M. A., Saiang, D., and Nordlund, E. (2012). Consideration of the rock mass property variability in numerical modelling of open stope stability. In Bergmekanikdag 2012: 12/03/2012-12/03/2012 (pp. 111-123), Stiftelsen bergteknisk forskning-Befo.

[11]. Idris, M. A., Nordlund, E., and Saiang, D. (2016). Comparison of different probabilistic methods for analyzing stability of underground rock excavations. The Electronic journal of geotechnical engineering. 21 (21): 6555-6585.

[12]. Seguini, M., and Nedjar, D. (2017). Modelling of soil–structure interaction behavior: geometric non-linearity of buried structures combined to spatial variability of soil. European Journal of Environmental and Civil Engineering. 21 (10): 1217-1236.

[13]. Tiwari, G., Pandit, B., Latha, G.M., and Babu, G.S. (2017). Probabilistic analysis of tunnels considering uncertainty in peak and post-peak strength parameters. Tunnelling and Underground Space Technology. 70: 375-387.

[14]. Tiwari, G., Pandit, B., Gali, M.L., and Babu, G.S. (2018). Analysis of tunnel support requirements using deterministic and probabilistic approaches in average quality rock mass. International Journal of Geo-mechanics. 18 (4): 1-20.

[15]. Heidarzadeh, S., Saeidi, A. and Rouleau, A. (2020). Use of probabilistic numerical modeling to evaluate the effect of geo-mechanical parameter variability on the probability of open-stope failure: a case study of the Niobec Mine, Quebec (Canada). Rock Mechanics and Rock Engineering. 53(3): 1411-1431.

[16]. Oreste, P. (2005). A probabilistic design approach for tunnel supports. Computers and Geotechnics. 32 (7): 520-534.

[17]. Fortsakis, P., Litsas, D., Kavvadas, M., and Trezos, K. (2011). Reliability analysis of tunnel final lining. Geotechnical Safety and Risk, ISGSR 2011, 409-418.

[18]. Langford, J. C., and Diederichs, M. S. (2013). Reliability based approach to tunnel lining design using a modified point estimate method. International Journal of Rock Mechanics and Mining Sciences. 60: 263-276.

[19]. Napa-García, G. F., Beck, A. T., and Celestino, T. B. (2017). Reliability analyses of underground openings with the point estimate method. Tunnelling and Underground Space Technology. 64: 154-163.

[20]. Kroetz, H. M., Do, N. A., Dias, D., and Beck, A. T. (2018). Reliability of tunnel lining design using the hyper-static reaction method. Tunnelling and Underground Space Technology. 77: 59-67.

[21]. Phoon, K. K., and Kulhawy, F. H. (1999). Characterization of geotechnical variability. Canadian Geotechnical Journal. 36 (4): 612-624.

[22]. Hoek, E. (1998). Reliability of Hoek-Brown estimates of rock mass properties and their impact on design. International Journal of Rock Mechanics and Mining Sciences. 35 (1):63-68.

[23]. Riedmuller, G. and Schubert, W. (1999). June. Rock mass modeling in tunneling versus rock mass classification using rating methods. In Vail Rocks, The 37th US Symposium on Rock Mechanics (USRMS). OnePetro.

[24]. Yu, X., Cheng, J., Cao, C., Li, E., and Feng, J. (2019). Probabilistic analysis of tunnel liner performance using random field theory. Advances in Civil Engineering.

[25]. Binder, K., and Heermann, D.W. (2010). Theoretical foundations of the Monte Carlo method and its applications in statistical physics. In Monte Carlo Simulation in Statistical Physics (pp. 5-67), Berlin, Heidelberg, Springer.

[26]. Hsu, S. C., and Nelson, P. P. (2006). Material spatial variability and slope stability for weak rock masses. Journal of Geotechnical and Geo-environmental Engineering. 132 (2): 183-193.

[27]. Mazraehli, M., and Zare, S. (2020). An application of uncertainty analysis to rock mass properties characterization at porphyry copper mines. Bulletin of Engineering Geology and the Environment. 79 (7): 3721-3739.

[28]. Fenton, G. A. (1999). Estimation for Stochastic Soil Models. Journal of Geotechnical and Geo-environmental Engineering. 125 (6): 470-485

[29]. Kim, H., and Major, G. (1978). Application of Monte Carlo techniques to slope stability analysis. In the 19th US Rock Mechanics Symposium.

[30]. Haldar, S., and Babu, G.S. (2008). Effect of soil spatial variability on the response of laterally loaded

pile in undrained clay. Computers and Geotechnics. 35 (4): 537-547.

[31]. Song, K.I., Cho, G.C., and Lee, S.W. (2011). Effects of spatially variable weathered rock properties on tunnel behavior. Probabilistic Engineering Mechanics. 26 (3): 413-26.

[32]. Lü, Q., Xiao, Z., Zheng, J., and Shang, Y. (2018). Probabilistic assessment of tunnel convergence considering spatial variability in rock mass properties using interpolated autocorrelation and response surface method. Geoscience Frontiers. 9 (6): 1619–1629.

[33]. Yu, X., Cheng, J., Cao, C., Li, E., and Feng, J. (2019). Probabilistic Analysis of Tunnel Liner Performance Using Random Field Theory. Advances in Civil Engineering.

[34]. Zhang, W., Han, L., Gu, X., Wang, L., Chen, F., and Liu, H. (2020). Tunneling and deep excavations in spatially variable soil and rock masses: A short review. Underground Space.

[35]. Cai, M., Kaiser, P.K., Tasaka, Y., Maejima, T., Morioka, H., and Minami, M. (2004). Generalized crack initiation and crack damage stress thresholds of brittle rock masses near underground excavations. International Journal of Rock Mechanics and Mining Sciences. 41 (5): 833-847.

[36]. Chen, D., Xu, D., Ren, G., Jiang, Q., Liu, G., Wan, L., and Li, N. (2019). Simulation of cross-correlated non-Gaussian random fields for layered rock mass mechanical parameters. Computers and Geotechnics. 112: 104–119.

[37]. Ching, J., Hu, Y G., Yang, Z.Y., Shiau, J.Q., Chen, J.C., and Li, Y.S. (2011). Reliability-based design for allowable bearing capacity of footings on rock masses by considering angle of distortion. International Journal of Rock Mechanics and Mining Sciences. 48 (5): 728–740.

[38]. Itasca. (2015). FLAC - Fast Lagrangian Analysis of Continua. Version 7.0. Minneapolis, Minnesota.

[39]. Jia, P., and Tang, C. A. (2008). Numerical study on failure mechanism of tunnel in jointed rock mass. Tunnelling and Underground Space Technology. 23 (5): 500-507.

[40]. Taghizadeh, H., Zare, S. and Mazraehli, M. (2020). Analysis of Rock Load for Tunnel Lining Design. Geotechnical and Geological Engineering. 38 (3): 2989-3005.

[41]. Xing, Y., Kulatilake, P. H. S. W., and Sandbak, L. A. (2018). Effect of rock mass and discontinuity mechanical properties and delayed rock supporting on tunnel stability in an underground mine. Engineering Geology. 238: 62-75.

[42]. Geodata (2016). Detailed design of Alborz main tunnel. Retrieved from Tehran-Shomal freeway project, Turin.

[43]. Hoek, E., Carranza-Torres, C., and Corkum, B. (2002). Hoek-Brown failure criterion-2002 edition. Proceedings of NARMS-Tac. 1 (1): 267-273.

[44]. Hoek, E., and Brown, E.T. (2019). The Hoek–Brown failure criterion and GSI–2018 edition. Journal of Rock Mechanics and Geotechnical Engineering. 11 (3): 445-463.

[45]. Hoek, E. and Diederichs, M.S. (2006). Empirical estimation of rock mass modulus. International Journal of Rock Mechanics and Mining Sciences. 43 (2): 203-215.

[46]. Yeglalp, T.M. and Mahtab, M.A. (1983). A proposed model for statistical representation of mechanical properties of rock. In the 24th US Symposium on Rock Mechanics (USRMS). OnePetro.

[47]. Grasso, P., Xu, S. and Mahtab, A. (1992). June. Problems and promises of index testing of rocks. In the 33rd US Symposium on Rock Mechanics (USRMS). OnePetro.

[48]. Hsu, S.C. and Nelson, P.P. (2002). Characterization of eagle ford shale. Engineering Geology. 67(1-2):169-183.

[49]. Gill, D.E., Corthésy, R., and Leite, M.H. (2005). Determining the minimal number of specimens for laboratory testing of rock properties. Engineering Geology. 78 (1-2): 29-51.

[50]. Sari, M. and Karpuz, C. (2006). Rock variability and establishing confining pressure levels. International Journal of Rock Mechanics and Mining Sciences. 43: 328-335.

[51]. Sari, M. (2009). The stochastic assessment of strength and deformability characteristics for a pyroclastic rock mass. International Journal of Rock Mechanics and Mining Sciences. 46 (3): 613-626.

[52]. Jiang, Q., Zhong, S., Cui, J., Feng, X.T., and Song, L. (2016). Statistical characterization of the mechanical parameters of intact rock under tri-axial compression: an experimental proof of the Jinping marble. Rock Mechanics and Rock Engineering. 49 (12): 4631-4646.

[53]. Sakurai, S. (1981). Direct strain evaluation technique in construction of underground opening. In the 22nd US Symposium on Rock Mechanics (USRMS), OnePetro.

[54]. Li, J., and Villaescusa, E. (2005). Determination of rock mass compressive strength using critical strain theory. In Proc. 40th US Symposium on Rock Mechanics, Anchorage, Alaska.

[55]. Kwasniewski, M., and Takahashi, M. (2010). Strain-based failure criteria for rocks: state of the art and recent advances. In ISRM International Symposium-EUROCK 2010, OnePetro.

[56]. Kong, X., Liu, Q., Pan, Y., and Liu, J. (2021). Stress redistribution and formation of the pressure arch

above underground excavation in rock mass. European Journal of Environmental and Civil Engineering, 25(4), 722-736.

[57]. Kavvadas, M. J. (2003). Monitoring and modelling ground deformations during tunneling. In Proceedings of the 11th FIG Symposium on Deformation Measurements.

[58]. Jiang, Q., Su, G., Feng, X. T., Chen, G., Zhang, M. Z., and Liu, C. (2019). Excavation optimization and stability analysis for large underground caverns under high geo-stress: a case study of the Chinese Laxiwa project. Rock Mechanics and Rock Engineering, 52(3), 895-915.

[59]. Russo, G. (2014). An update of the "multiple graph" approach for the preliminary assessment of the excavation behavior in rock tunneling. Tunnelling and underground space technology, 41, 74-81.

تحلیل پایداری تصادفی تونل‌ها با در نظر گرفتن تغییرپذیری فضایی خصوصیات توده‌سنگ

مسعود مزرعه لی[1*]، شکراله زارع[1] و موسی آدبابیو ادریس[2]

۱-دانشکده مهندسی معدن، نفت و ژئوفیزیک، دانشگاه صنعتی شاهرود، شاهرود، ایران

۲- بخش مهندسی معدن و ژئوتکنیک، دانشگاه صنعتی لولئا، لولئا، سوئد

ارسال ۲۰۲۱/۱۰/۲۰، پذیرش ۲۰۲۱/۱۲/۱۱

* نویسنده مسئول مکاتبات: mazraehli.m@shahroodut.ac.ir

چکیده:

هدف از این مطالعه ارائه رویکردی برای تحلیل پایداری احتمالاتی تونل‌ها با در نظر گرفتن ناهمگونی خصوصیات ژئومکانیکی است. یک رویه تصادفی برای منظور کردن تغییرپذیری در ویژگی‌سنجی خصوصیات توده‌سنگ به کار گرفته شد. روش عددی تفاضل محدود با تکنیک شبیه‌سازی مونت کارلو ممزوج گردید تا خاصیت تصادفی خصوصیات توده‌سنگ در مدل‌سازی در نظر گرفته شود. به‌علاوه، یک تابع عملکرد خاص مبتنی بر تغییرشکل‌های مجاز توده‌سنگ به‌منظور بررسی سرویس‌دهی تونل تعریف شد. نتایج تحلیل‌های احتمالاتی و یقینی به‌منظور اعتبارسنجی با اندازه‌گیری‌های برجا مقایسه گردید. نتایج نشان از این دارد که بیشترین جابجایی‌ها در هر دوی تحلیل‌های احتمالاتی و یقینی در کف تونل رخ می‌دهد. در طرف مقابل، کمترین تغییرشکل‌ها در دیواره‌های کناری ثبت شده اند. با استفاده از تابع عملکرد، احتمال وقوع ناپایداری در کف، سقف و دیواره‌ها معادل ۱۰۰، ۶۸/۸، ۱۶/۲ و ۲۰/۹ درصد ارزیابی شده است. مقایسه مقادیر همگرایی اندازه‌گیری و محاسبه‌شده نشان از این دارد که تحلیل یقینی مقادیر جابجایی را کمتر از مقدار واقعی تخمین می‌زند در حالی‌که مقادیر میانگین مدل-های تصادفی به مقادیر اندازه‌گیری‌شده بسیار نزدیک بوده اند. بنابراین، رویکرد پیشنهادی را می‌توان به‌عنوان یک روش قابل اعتماد در مقایسه با روش یقینی مرسوم در نظر گرفت.

کلمات کلیدی: حفریات زیرزمینی، تحلیل پایداری احتمالاتی، تغییرپذیری خصوصیات توده‌سنگ، روش تفاضل محدود، شبیه‌سازی مونت کارلو.